

## **The Effect of Pretreatment and Thin Layer Sulfuric Acid AC Anodization on The Corrosion Resistance of 6063 Aluminium Alloys**

*Feriha Serçelik, Research and Development Centre of ARÇELİK A.Ş., Çayırova, Istanbul -TURKEY*

*Ali Fuat Çakır, Istanbul Technical University, Department of Metallurgy and Materials Engineering,  
80626 Ayazağa, Istanbul - TURKEY*

*Mustafa Ürgen, Istanbul Technical University, Department of Metallurgy and Materials Engineering,  
80626 Ayazağa, Istanbul - TURKEY*

*David R. Gabe, IPTME, Loughborough University, LE11 3TU, UK*

The formation of a thin oxide film (4 - 5  $\mu\text{m}$ ) on aluminium alloys by anodization, as a substitute for chromate pretreatment before powder coating, is a viable alternative. Thin anodised layers provide both good adhesion to the coating and protection to aluminium alloys. The aim of this work is to investigate the effect of surface pretreatments such as alkaline etching and nitric acid desmutting on the corrosion performance of AC anodised thin oxide films on commercial 6063 aluminium alloys. The corrosion of DC and AC anodized layers and the effect of molybdate ions added into the AC anodization solution were also investigated.

### **For more information, contact:**

Prof. Dr. Ali Fuat Çakır  
Istanbul Technical University,  
Department of Chemical and Metallurgical Engineering  
80626 Ayazağa, Istanbul / TURKEY

Phone : \*\*90-212 285 3528

FAX : \*\*90-212 285 2925

E-mail : [afcakir@itu.edu.tr](mailto:afcakir@itu.edu.tr)

## Introduction

The industrial use of powder coated or painted aluminium alloys has been steadily increasing. Powder coating or painting of aluminium substrates provide a decorative appeal to the surface and also improves its corrosion resistance.

Aluminium alloys are chromate passivated prior to powder coating to provide adhesion of coating to the substrate. Recent surveys have shown that there are increasing evidence of filiform corrosion and underfilm corrosion of chromated and painted or powder coated aluminium products in environments combining marine and industrial atmospheres<sup>1</sup>. Hence, chromate conversion coatings are not sufficient in preventing filiform corrosion completely. Additionally, hexavalent chromium is not safe for humans as well as for the environment and extensive work is carried out to replace it with safer substitutes<sup>2</sup>.

Filiform corrosion (FFC) which occurs at the metal/coating interface affects decorative appearance of coated materials. Due to an abrupt increase of filiform corrosion failures in Western Europe, recent studies have focused on the causes and remedies for it<sup>2, 3</sup>. The most important factors affecting filiform corrosion are adhesion between coating and substrate, defects in the coatings and corrosion resistance of the substrate or pretreated surface<sup>2, 4-7</sup>.

The formation of a thin oxide film produced by anodisation on aluminium alloys as an underlayer before powder coating is a potential candidate to substitute chromate pretreatment<sup>8</sup>. It has been also reported that a thin layer of direct current (DC) anodised oxide film remarkably improved filiform corrosion resistance of powder coated aluminium alloy substrate<sup>7-9</sup>. Thin anodised layers provide both good adhesion to the coating and protection to aluminium alloys.

Alternating current (AC) anodizing of aluminium substrate is an old process<sup>10-26</sup> but the yellow coloring of the oxide layer due to sulfate reduction and the odour due H<sub>2</sub>S evolution hampered its decorative appeal<sup>10-12, 16, 17, 24</sup>. Thin layer AC anodized layer will not have similar disadvantages if used as an underlayer for powder coating. AC layers can easily be made more porous which will aid adhesion to the powder coating.

Molybdate ions have been widely exploited as a promising corrosion inhibitor<sup>27-29</sup>, and a passivating agent to replace environmentally hazardous hexavalent chromium. Besides, addition of molybdate ions into sulphuric acid solutions

during alternative current (AC) anodization eliminates yellowish coloration of the oxide films and intensive H<sub>2</sub>S odour<sup>30</sup>. If molybdate ions are also incorporated into the oxide layer during AC anodization, additional passivating advantages of these ions could improve the corrosion resistance of thin AC anodized oxide layers under powder coatings.

Therefore, the aim of this work was to investigate the effect of surface pretreatments such as etching and desmutting on the corrosion performance of AC anodised thin oxide films on commercial 6063 aluminium alloys and also to examine the effect of molybdate ion additions to the anodisation solution on the corrosion performance of the thin oxide layers. It supplements also the previously published works by the authors<sup>31-34</sup>

The experiments were carried out with commercial (6063) aluminium alloy samples. They were alkaline etched, desmutted in dilute nitric acid and DC and AC anodised in H<sub>2</sub>SO<sub>4</sub> solutions. 0.01N HCl solution was used for corrosion testing of anodized samples. Electrochemical impedance spectroscopy (EIS), scanning electron microscope (SEM) and copper decoration technique were used to examine and characterise the surfaces.

## Experimental

The aluminium alloy was commercial 6063 alloy (0.158%(w) Fe, 0.36% Si, 0.365% Mg) which is widely used as substrate for powder coating as well as for anodization. The alloy was submitted to T5 heat treatment. Experimental samples (40 x 40 x 1 mm in size) were cut from the extruded strips (1000 x 50 x 1 mm. in size).

The following experiments were carried out:

- Etching:** Samples were degreased in 5% Na<sub>2</sub>CO<sub>3</sub>+5%Na<sub>3</sub>PO<sub>4</sub> at 55 °C, washed with distilled water, and then etched in 5%NaOH solution at 55 °C, for 3 min., 5 min. and 10 min. to determine the effect of etching on the Al matrix and the particles it contains. The smut layer produced following etching was removed ultrasonically in distilled water.
- Desmutting:** Some of the 5 min. etched samples were desmutted in 33% HNO<sub>3</sub> for 3 min., 5 min. and 10 min. to determine the effect of desmutting on the Al matrix and the particles it contains.
- AC Anodization:** AC anodisation was carried out in 10% H<sub>2</sub>SO<sub>4</sub> solution at 20 °C at constant voltage of 20 and 25 V<sub>rms</sub> by using an

autotransformer (10 A, 200 V and a frequency of 50 Hz from the main) as power supply.

Before anodisation, the as-received samples were subjected to the following treatments: degreasing in 5%  $\text{Na}_2\text{CO}_3$ +5% $\text{Na}_3\text{PO}_4$  at 55 °C, etching in 5% NaOH and desmutting in 33%  $\text{HNO}_3$  at room temperature, each for 5 minutes. After each treatment the samples were thoroughly rinsed with distilled water. All samples were anodised to produce 4-5  $\mu\text{m}$  thick oxide films.

In order to investigate the effect of molybdate ions on the anodization and on the properties of oxide layer, sodium molybdate was added to anodization electrolyte in the concentration of 5.7, 8 and 40 g/l.

- d) **DC Anodization:** DC anodisation was also conducted in 10%  $\text{H}_2\text{SO}_4$  solution at 20 °C. at constant voltages of 20 and 25 V. Preanodization treatments were similar to AC anodization.

The following experimental techniques were used to evaluate the various test results:

- a) **Scanning Electron Microscope (SEM)** equipped with Energy Dispersive X-Ray Spectroscopy (EDS) for chemical analysis was used to examine the sample surfaces before and after various experiments (Jeol 5410).

- b) **Electrochemical Impedance Spectroscopy (EIS)** was the major technique applied to investigate the behaviour of etched and desmutted samples in 0.1M NaCl and anodized samples in 0.01N HCl at room temperature. EIS is an extensively used technique to investigate the behaviour of anodized and nonanodized aluminium alloy surfaces<sup>35-42</sup>.

All EIS measurements were carried out at  $E_{\text{corr}}$ , with an AC potential amplitude of 10 mV and in the frequency range of  $10^{-2}$ - $10^5$  Hz. The EIS set up consisted of EG&G 273 model potentiostat, 5315 preamplifier, 5301 lock-in amplifier and a computer. The cell used for experiments was open to air and the exposed area of the sample for test was 8  $\text{cm}^2$ . All potentials were measured with respect to saturated calomel electrode.

Two types of EIS measurements were carried out: a) As received, etched and desmutted samples were introduced into 0.1 M NaCl solutions b) To compare the corrosion performance of anodised samples, they were immersed for 8 days into 0.01 N HCl solution. EIS experiments were conducted at the end of 20 min, 1 h, 20 h, 24, h, 48 h and 8 days.

- c) **Copper decoration** technique was applied to the anodised and nonanodized aluminium alloy

surfaces to identify the electrochemically active particles and regions<sup>43</sup>. Two types of copper decoration were used: a) For non anodised surfaces, simple immersion of the sample into copper decoration solution was conducted. The copper decoration procedure was as follows: The sample was kept in 100ml of 0.1 M NaCl solution for 15 min.. Then 0.5 ml of  $\text{Cu}^{++}$  solution ( 35 g/l  $\text{CuSO}_4 \cdot 5\text{H}_2\text{O}$ ) was added into the beaker at the end of 15 min.. After holding the sample for 60 sec. in the  $\text{Cu}^{++}$  ions containing solution, it was removed from the beaker and rinsed with distilled water then dried in cool air current. Decorated surfaces were examined with SEM. b) For anodized surfaces, modified electrochemical decoration technique was applied. Decoration was carried out immediately following anodisation (without drying). The copper decoration solution contained 100 ppm  $\text{Cu}^{++}$  at pH=1 (fixed with HCl). Using the specimen as a cathode, anodised aluminium alloy surfaces were decorated by applying a 2 V cell voltage for 20 sec., then the decorated samples were examined with SEM. The technique was a modified version of the standard test (ISO 2085-(1976)), which produced extensive decoration and made a meaningful interpretation impossible.

- d) **Corrosion tests:** To compare the corrosion performance of anodised samples they were immersed for 8 days into 0.01 N HCl solution. HCl solutions are widely used to inoculate filiform corrosion<sup>9</sup> (DIN 65472). The samples anodised and exposed to 0.01 N HCl solution were also examined with SEM to determine the effect of corrosive solution to oxide layer.

## Results and Discussions

### *SEM Examination of mechanically polished samples*

In order to determine the distribution, size and approximate composition of the particles in the as-received alloy, a mechanically polished sample was examined with SEM. A homogenous distribution of particles in various sizes was observed. Mainly two types of particles were identified from the X-ray maps and electron images: a) particles with Mg and Si and b) particles with Al, Fe and Si. Al-Fe-Si particles were in majority and had acicular shape with a length of 7-8  $\mu\text{m}$  and a width of 0.5-1  $\mu\text{m}$ . Fe:Si ratio (% a) of Al-Fe-Si particles always fell into the two ranges: one group was in the range of 0.9-1.3, the other one 1.7-3.

### *Effect of etching time (3min., 5min. and 10 min.) in 5% NaOH solution at 55 °C*

Etching in NaOH solution produced a smut layer at the alloy surface where Mg and Si were accumulated. It is well known that Mg-Si particles in aluminium alloys dissolve in caustic solutions<sup>44, 45</sup>. Hence, during etching they dissolved but their dissolution products remained in the smut layer. When the smut layer was ultrasonically cleaned in distilled water the EDS analysis of particles at the alloy surface indicated to substantial decrease in the particles containing Mg-Si and also selective dissolution of Al from Al-Fe-Si particles. After 10 min. etching although the ratio of Fe/Si remained constant Al/(Fe+Si) ratio decreased from about 4.34 in as received samples to 2.2 in etched surfaces. However density of particles on etched surfaces were not very different than the as received samples.

The EIS data of the etched samples obtained, following ultrasonic cleaning in distilled water, in 0.1M NaCl solutions showed that surface resistance of 6063 aluminium alloy decreased ( $\approx 450 \text{ Ohm.cm}^2$  for 5 min. etched sample,  $\approx 230 \text{ Ohm.cm}^2$  for 10 min etched sample) with etching time as shown in Figure 1.

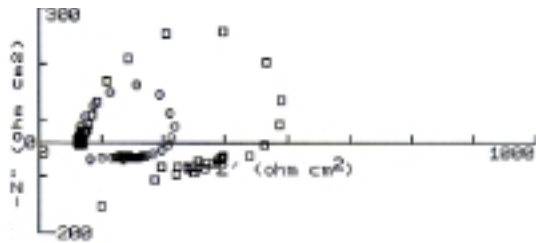


Figure 1: Nyquist diagrams of EIS data of etched (in %5 NaOH solution at 55 °C) 6063 aluminium alloy surfaces obtained in 0.1 N NaCl, as a function of etching time a) (□): 5 min. and (O): 10 min.. (samples ultrasonically cleaned in distilled water before immersing in NaCl solution)

During etching, both Al in the matrix and in the particles dissolved selectively. Dissolution of Al matrix may increase the exposed surface area of intermetallic particles with etching time. Particles containing Fe and Si are nobler than Al matrix in chloride containing solutions<sup>46</sup>. When the etched samples were immersed into chloride containing solutions, increased exposed area of particles may increase the galvanic current between the particles and the matrix, hence the surface resistance decreases. Selective dissolution of Al in the particles during etching causes Fe enrichment on

the surface of Al-Fe-Si particles as found in this work and also reported by Nisancioglu et al<sup>47,48</sup>. Higher etching time increases Fe enrichment on the particle surfaces, resulting also in an increase of the galvanic current. As a result, the surface resistance of the etched samples may decrease.

### *Effect of desmutting time (3min., 5 min. and 15 min.) in 33% HNO<sub>3</sub> solution*

The particle population on the desmuted surfaces did not change remarkably as a function of treatment time. However, the x-ray mapping of the samples revealed that the number of ternary Al-Fe-Si particles decreased with increasing desmutting time. Furthermore, the majority of the particles on the 15 min. desmuted sample surfaces were Si rich. Several large ternary Al-Fe-Si particles with a dissolved region around them were also detected. In order to determine active particles electrochemically, the copper decoration technique was applied to samples following desmutting treatment. In this technique, copper ions reduce at the cathodic regions and deposit as metallic copper, taking electrons produced by the dissolution of active sites.

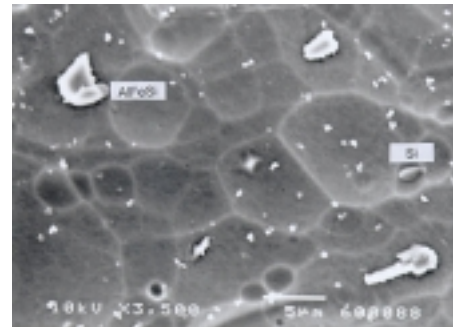


Figure 2: Copper decorated AlFeSi and undecorated Si-rich particles on the surface of the desmuted samples in 33% HNO<sub>3</sub> solutions after 5 min. etching in 5 % NaOH (55°C).

Copper deposited around all particles with Fe (Figure 2) indicated to electrochemically active sites. Density of copper decorated sites was very high on the surfaces desmuted for a short time (3 min.) and decreased with increasing desmutting time indicating to a decrease in the density of particles containing Fe. Chemical analysis of the desmutting solutions revealed the presence of iron in the solution while no Fe could be detected in a freshly prepared desmutting solution. Uhlig<sup>49</sup> reported that pure aluminium has lower dissolution rate than pure iron in 30-50% HNO<sub>3</sub> solutions, which supported our findings. These results

indicate to selective dissolution of Fe in Fe containing particles during desmutting.

Only Si and Al were identified in the majority of the particles after long period of desmutting treatment (15 min.) Copper deposition was not observed on or around the particles with only Si. It is expected that these sites could act as cathode when coupled galvanically with the Al matrix, since potential of Si is nobler than that of Al matrix<sup>46</sup>. However, an electrochemically passive  $\text{SiO}_2$  layer could form easily on Si in aqueous solutions (EDS analysis of some Al-Fe-Si particles, following 15 min. desmutting showed drastic decrease in Fe content, almost to 0%, and substantial increase in O, around to 40%). Nisancioglu et.al<sup>47</sup> claimed that such electrochemically passive layer suppresses the rate of cathodic reactions and lowers the galvanic effect of Si remarkably. Hence, particles with only Si did not create electrochemically active sites.

The resistance of the surfaces in chloride solution increased with increasing desmutting time ( $\approx 650 \Omega \cdot \text{cm}^2$  for the 5 min desmutted sample and  $\approx 1250 \Omega \cdot \text{cm}^2$  for the 15 min desmutted sample) in 0.1 M NaCl solution. This increase is most likely due to the oxidation of alloy surface in nitric acid solution and to the variations of intermetallic particle composition at their surfaces due to selective dissolution of active Fe from the particle. Copper decoration experiments had shown that the number of active sites around the particles with Fe had also decreased. This decrease in the electrochemically active sites probably decreased the galvanic activity, hence increasing the resistance of surfaces in 0.1 M NaCl solutions.

#### *Effect of etching and desmutting on the AC anodised films*

The AC anodised film thicknesses were approximately  $5 \mu\text{m}$  and were produced by 10 min. anodization ( at  $20 \text{ V}_{\text{rms}}$  and  $20^\circ\text{C}$  ). Anodized films were not thick enough to cover large second phase particles. However, the oxide film was grown coherently with these particles and dissolution region around them was not observed. Small particles containing only Si were embedded completely in the film. Copper decoration studies conducted in HCl containing weak acidic solution revealed that all particles containing Fe were active. Copper deposited on the Fe containing particles (Figure 3). No deposition was determined on or around only Si containing particles, similar to the desmutted surfaces.

EIS experiments showed that the resistance of anodized samples were affected by surface pretreatment. When the desmutting treatment in 33%  $\text{HNO}_3$  was kept longer (eg. 15 min.) the surface resistance of anodized samples became higher. The oxide film resistance of anodized surfaces became lower if desmutting was shorter, due to higher density of the Fe rich particles. On these surfaces, the density of copper decorated

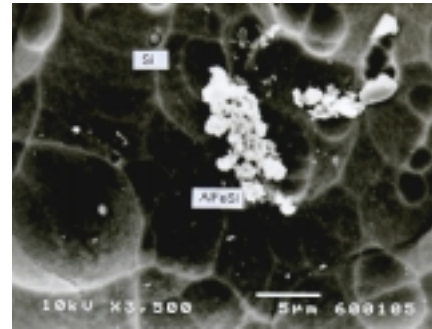


Figure 3: Electron micrograph of the surface of an anodized sample in 10%  $\text{H}_2\text{SO}_4$  at  $25 \text{ V}_{\text{rms}}$  and at  $20^\circ\text{C}$  showing copper decorated AlFeSi and undecorated Si-rich particles

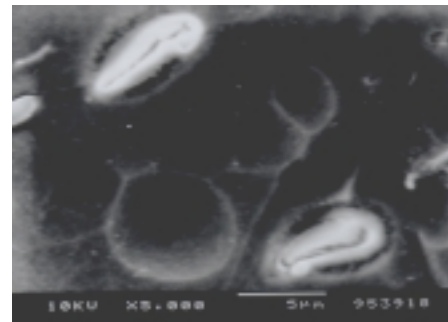


Figure 4: Electron micrograph of the surface of an anodized sample in 10%  $\text{H}_2\text{SO}_4$  at  $25 \text{ V}_{\text{rms}}$  and at  $20^\circ\text{C}$ , showing particle/oxide film interface

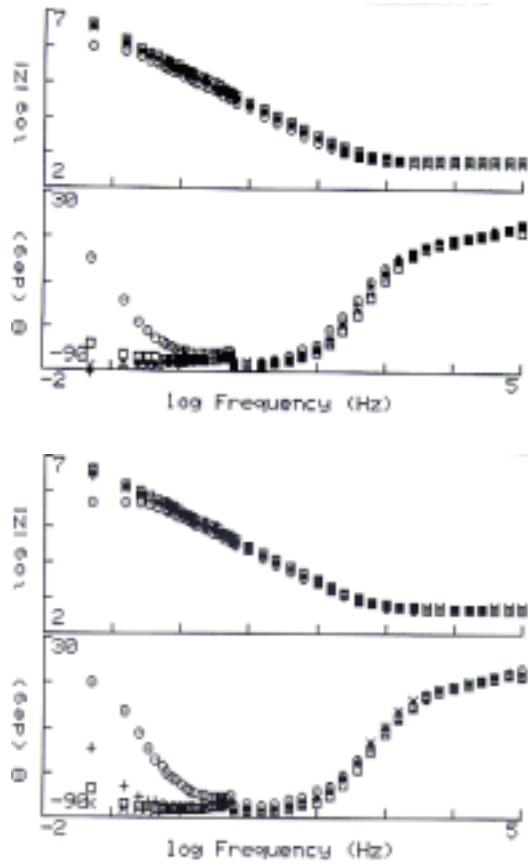
spots, indicating to the density of Fe containing particles, was higher than those desmutted for longer time.

#### *AC anodisation in 10 % $\text{H}_2\text{SO}_4$ solution at $20^\circ\text{C}$*

Current density was constant during anodization at constant potential of  $25 \text{ V}_{\text{rms}}$ .  $5 \mu\text{m}$  thick oxide films were produced in about 3-4 minutes.  $5 \mu\text{m}$  thick oxide film was not enough to cover all second phase particles completely (SEM examination); but oxide film growth was coherent with the particles (Figure 4 ).

Figure 5: Bode Plots of EI data of the AC anodized samples in a) 10%  $\text{H}_2\text{SO}_4$ , b) 10%  $\text{H}_2\text{SO}_4 + 8 \text{ g/l}$

$\text{Na}_2\text{MoO}_4$  exposed to 0.01 N HCl solution for ( $\square$ ):1, ( $\times$ ): 20, (+): 24, ( $\odot$ ): 48 hours.



EI spectras were obtained with AC anodised samples at the end of 1, 24 and 48 hours in 0.01 N HCl solution are showed in Figure 5.

No remarkable change on the plots was observed in 24 hours. The measured impedance spectra of an unsealed porous oxide film obtained with present commercial instrumentation consist mainly of a contribution from the barrier layer capacitance rather than porous oxide layer<sup>35</sup>. Therefore, no information on pore size, cell volume, cell thickness can be obtained directly from EIS measurements in aqueous solutions<sup>51</sup>. However, it may be possible to compare total corrosion performance of the anodised films by comparing changes appeared at low frequencies on the EI spectra<sup>35</sup>. Assuming the bulk oxide dielectric constant ( $\epsilon$ ) is 12, the barrier layer thickness was calculated<sup>36, 51</sup> from the measured EIS data obtained at the end of 20 minutes, 24 and 48 hours. Table 1 summarises the results of the various barrier layer thickness calculation of AC (in plain and molybdate containing electrolytes) and DC anodized oxide layers. N at the table refers to the AC anodized sample attached to neutral and L to

live leads. Table 2 includes the thicknesses of various oxide layers, measured by conventional way, before the EI measurements.

Calculated thicknesses for the N and L poles were 205 Å and 211 Å respectively. These values are close to the value of 190 Å from the literature<sup>52</sup> which is estimated by using the relationship of 7.6 Å barrier oxide growth per volt of anodizing voltage of barrier growth rate in sulfuric acid solutions for AC anodization of 2024 aluminium alloy.

Table 1: Barrier layer thicknesses of AC and DC anodized (in % 10  $\text{H}_2\text{SO}_4$  at 20°C and 25  $V_{\text{rm}}$ ) 6063 aluminium alloys calculated from the impedance data obtained in 0.01 N HCl solution, as a function of time: 20 min., 24 and 48 hours.

	Barrier Layer Thickness (Å)					
	20 min.		24 hours		48 hours	
	N	L	N	L	N	L
Anodized in %10 $\text{H}_2\text{SO}_4$ (AC)	202	211	158	151	134	108
Anodized in %10 $\text{H}_2\text{SO}_4$ + 8g/l $\text{Na}_2\text{MoO}_4$ (AC)	203	217	162	163	148	63
Anodized in %10 $\text{H}_2\text{SO}_4$ (DC)	204		173		93	

A remarkable change on the Bode plot occurred at the end of 48 hours; total impedance of the oxide film decreased from above  $10^7$  Ohms.cm<sup>2</sup> to approx.  $10^6$  Ohms.cm<sup>2</sup> for both samples produced at L and N poles. At the same time barrier layer capacitance increased indicating to a decrease in the thickness of the barrier layer ( to 158 Å for N and 151 Å for L samples). The substantial decrease in the impedance may also indicate to the contribution of the dissolution of porous layer. This

Table 2: Anodic oxide film thickness of the AC and DC anodized samples in 10%  $\text{H}_2\text{SO}_4$  solutions prior



to EIS experiment and after exposure to 0.01 N HCl solution for 48 hours.

Oxide film thickness ( $\mu\text{m}$ )	Prior to EIS		After 48 hours	
	N	L	N	L
% 10 $\text{H}_2\text{SO}_4$ (AC)	4.8	5	4.2	4.7
% 10 $\text{H}_2\text{SO}_4$ (DC)	5.2		3.1	

interpretation was supported by thickness measurement of oxide layer after 48 hours immersion into acidic chloride solution (Table 2).

EI spectra changed remarkably on the 8th day indicating a bare aluminium surface. Thickness measurement and SEM examination also showed that the AC oxide film had dissolved completely. The bare alloy surface was populated with deep pits exhibiting crystallographic dissolution morphology.

Active sites on anodised surfaces were determined by using copper decoration technique. Fe-Si containing particles were copper decorated but only Si containing particles were not (Figure 3). Also only some of the Al-Fe-Si particles were covered with copper; indicating the formation of a protective layer on the non-decorated particles.

#### *AC anodisation in molybdate ion containing 10% $\text{H}_2\text{SO}_4$ at 20 °C*

Addition of  $\text{Na}_2\text{MoO}_4$  to 10% sulphuric acid solution increased the anodisation rate and eliminated the evolution of sulphurous smell. At a given anodisation voltage (25  $\text{V}_{\text{rms}}$ ) and temperature (20°C) anodisation rate increased with increasing  $\text{Na}_2\text{MoO}_4$  concentration. Current was not stable during anodisation and it increased to very high values during the first minute, then decreased gradually in all solutions containing various molybdate concentration.

Many spots were observed on the oxide film produced in molybdate containing sulphuric acid solutions; they were Al-Fe-Si particles with a poor coherency to the oxide film (Figure 6). Also, other roselike clusters with different structure than the oxide film were observed. However, EDS analysis did not reveal any composition difference between the oxide film and these clusters.

The presence of molybdate could not be identified unambiguously by EDS since sulphur-K and molybdenum-L peaks overlapped at an accelerating

voltage of 15 kV. EDS analysis at a higher accelerating voltage ( $\text{Mo}_{\text{K}\alpha}$  at 30 kV) revealed some Mo (0.62-1.29 % (w)).

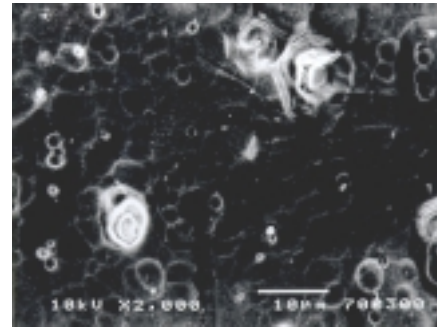


Figure 6: Rose-like nodules in the oxide films produced by AC anodization in 10 %  $\text{H}_2\text{SO}_4$ +8g/l  $\text{Na}_2\text{MoO}_4$  at 25  $\text{V}_{\text{rms}}$  and 20°C, with poor coherency of intermetallic/ oxide interface.

EI spectra's of AC films formed both in molybdate free and molybdate containing sulphuric acid solutions were similar in 1 hour. The barrier layer thicknesses for L and N samples calculated from the spectra were approx. 217 Å and 203 Å respectively. First changes on the EI spectra of anodised films obtained in molybdate containing sulphuric acid appeared at the end of 20 hours, and in some cases 24 hours (Figure 5). At the end of 46 hours immersion into acidic chloride solution, decrease in the total impedance of anodized layer was higher than that of only sulphuric acid anodised films indicating important dissolution of porous film. Resistances of the N and L samples were  $\approx 5 \times 10^5$  and  $10^5$  Ohms. $\text{cm}^2$  respectively. However, dissolution of barrier layer thickness for N and L samples were quite different (148 Å and 63 Å (!) for N and L samples respectively). Except the L pole, the rate of decrease was comparable to the rate of barrier layer thickness decrease of the only  $\text{H}_2\text{SO}_4$  anodized layers.

These results may be explained in two ways: molybdate ions may alter either porous layer properties or the resistivity properties of the barrier oxide layer, which may then cause such changes in total resistance of the system.

After 8 days of exposure to 0.01 N HCl solution, the oxide film dissolved completely and pits appeared on the substrate. However, the pits had a different morphology than those formed on the substrate anodised in molybdate free sulphuric acid solutions. They had crystallographic inner surface morphology but were larger and shallower. It is well documented that the presence of molybdate ions has similar influence on the pitting of stainless steels<sup>27</sup>.

On the other hand, roselike clusters with a different structure than oxide film did not dissolve even in 8 days but the oxide film surrounding these clusters dissolved faster after 20 hours exposure and during copper decoration.

Copper decoration results were very similar to the sulphuric acid anodised samples in terms of decorated particles. Similarly, Al-Fe-Si particles were copper decorated while only Si containing particles were not. Larger number of Al-Fe-Si particles were decorated compared to the molybdate free sulphuric acid anodised samples. On the other hand, although a dissolution region was observed around rose like clusters, copper decoration was not observed at these regions.

### *DC anodisation in 10 % H<sub>2</sub>SO<sub>4</sub> solution at 20 °C*

Anodization at 25 V produced 5 µm thick oxide films in about 3-4 minutes. SEM examination of the oxide films revealed that the number of uncovered particles in oxide layer was more in DC anodized samples than AC anodized alloys.

EI spectras were also obtained with DC anodised samples at the end of 1, 24 and 46.5 hours in 0.01 N HCl solution. No remarkable change on the plots was observed in 24 hours.

Calculated thickness of the barrier layer of DC anodized sample was 204 Å. This value is close to the value of 220 Å from the literature<sup>52</sup> which is estimated by using the relationship of 8.8 Å barrier oxide growth per volt of anodizing voltage of barrier growth rate in sulfuric acid solutions for DC anodization for 2024 aluminium alloy.

Remarkable change to the Bode plot occurred at the end of 48 hours, total impedance of the oxide film decreased from above 10<sup>7</sup> Ohms.cm<sup>2</sup> to approx. 10<sup>5</sup> Ohms.cm<sup>2</sup>. Barrier layer thickness decreased to 93 Å. The thickness of oxide layer during the same period decreased 40 % which was greater than the dissolution of AC anodized oxide layers (%13 N pole, %7 L pole) in the same solution.

After 8 days of immersion, the surface oxide also dissolved completely.

All Al-Fe-Si particles were fully covered with copper after copper decoration tests.

## **Conclusions**

1. Etching of aluminium alloy 6063 in 5% NaOH solution dissolved both the aluminium matrix

and the particles with Mg and Si and increased the exposed surfaces of Al-Fe-Si intermetallics.

2. Aluminum in the Al-Fe-Si particles were preferentially dissolved by alkaline etching solution.
3. Desmutting of etched surfaces in 33% HNO<sub>3</sub> dissolved Fe selectively, leaving mostly Si behind in Fe-Si containing particles and copper is deposited around Fe containing particles, indicating their electrochemically active behaviour.
4. The surface resistance (determined by EIS) of the etched samples decreased considerably with etching time while it increased with desmutting time.
5. Desmutting and etching affected the resistance of AC anodized surfaces. The anodized samples desmutted for longer time exhibited higher surface resistance in 0.01 N HCl due to the formation of protective oxide layer on the aluminium matrix and to lower density of the Fe rich active particles.
6. AC anodized oxide films had lower number of active Fe containing particles compared to DC anodized layers.
7. During A.C. anodisation the presence of molybdate ion in 10% H<sub>2</sub>SO<sub>4</sub> solution increased the oxide film formation rate and prevented the evolution of sulphurous smell. Oxide film formation rate increased with increasing molybdate ion concentration.
8. Molybdate addition to anodisation solution did not improve the resistance of the oxide films to 0.01 N HCl solutions. After 48 hours immersion in 0.01N HCl solution barrier layer resistance of the oxide films formed in molybdate containing sulphuric acid solutions decreased more than the resistance of the oxide films formed in molybdate free sulphuric acid solution. Similarly, porous side of the oxide film formed in molybdate containing anodization solution. dissolved faster in acidic chloride media
9. The pits developed at the aluminium alloy (6063) surface, following the dissolution in 0.01 N HCl solution of oxide layer produced in molybdate containing sulphuric acid solution, was large and shallower when the oxide film was compared to the substrate of oxide film formed in molybdate free solution.
10. Molybdate containing sulphuric acid anodised oxide films had more active defect sites such as incoherent Al-Fe-Si particle/oxide interfaces, and roselike clusters.



## Acknowledgement

The authors kindly acknowledge the valuable contributions of British Council and NATO SFS-TU-Coatings Project to this investigation.

## References

1. K. Nişancioğlu, O. Lunder, and H. Holtan, *Corrosion*, **41**, 5, 247 (1985)
2. J.E. Pietschmann and H. Pfeifer, *Aluminium*, **70**, 1/2, 82 (1994)
3. J.E. Pietschmann and H. Pfeifer, *Aluminium*, **69**, 11, 1081 (1993)
4. H. Leth-Olsen and K. Nisancioglu, *Corrosion*, **53**, 9, 705 (1997)
5. H. J. W. Lenderink, *Filiform Corrosion of Coated Aluminium Alloys*, PhD thesis, Delft University of Technology, The Netherlands, pp 175, (1995)
6. Rudolph, and W. D. Kaiser, *Aluminum*, **72**, 10, 726 (1996)
7. A. Rudolph and W. D. Kaser, *Aluminum*, **72**, 11, 832 (1996)
8. T.E. Gomez, and I De Miguel Lopez, *Proceedings of Aluminium 2000*, **3**, p. 175 (1996)
9. J.E Pietschman, and H. Pfeifer, *Aluminium*, **69**, 11, 1019 (1993)
10. P. Sacchi, *Trans. Inst. Metal Finishing*, **40**, 229. (1963)
11. J. M. Kape, *Metal Finishing Journal*, April, 80 (1974)
12. J.M. Kape, Patent Specification, 1 439 933 (1976).
13. D.R Gabe and I.H. Dowty, *Surface and Coatings Technology*, **30**, 303 (1987)
14. D.R Gabe and J.M Kape, *Proceedings of The 4<sup>th</sup> International Congress On Surface Technology*, p 355 (1987)
15. M.A Barbosa, D.R Gabe and D.H Ross, I., Shutherland, *Journal of Appl. Electrochem.*, **19**, 82 (1989)
16. V. Balasubramanian, S. John and B.A. Shenoi, *Surface Technology*, **19**, 293, (1983)
17. J.M. Kape, *Trans. Inst. Metal Finishing*, **63**, 90. (1985)
18. W.E Cooke, *Plating*, March, 239 (1975)
19. J.A. Kneeshaw and D.R. Gabe, **62**, 59 (1984)
20. D.A.L Nicklen and D.R Gabe, *Surface Technology*, **7**, 353 (1979)
21. D Eyre and D.R Gabe, *Trans. Inst. Metal Finishing*, **57**, 38 (1979)
22. H. Zahavi, H. Kerbel, O. Korotkina, *J. Electrochem. Soc.*, **129**, 1572 (1982).
23. V. Balasubramanian, S. John, B. A. Shenoi, *Surface Technology*, **19**, 293. (1983)
24. Mita I., *Keakyu Hokoku Tokyo Toritsu Kogyo Giyutsu Seata*, **13**, 133, (1984)
25. A.P Gruar and D.R Gabe, *Trans. Inst. Metal Finishing*, **63**, 1, 1 (1984)
26. D.R Gabe, *Trans. Inst. Metal Finishing*, **65**, 152. (1987)
27. M. Ürgen, and A.F. Çakır, *Corr. Sci.*, **32**, 8, 841 (1991)
28. F Sertçelik, M. Ürgen and A.F Çakır, *Proceedings of Eurocorr'91*, **I**, p 441 (1991)
29. C. D. Wilcox and D.R Gabe, *Korozyon*, **3**, 1, 3 (1991)
30. J. M. Kape, *Trans. Inst. Metal Finishing*, **55**, 25 (1977)
31. F. Sertçelik, A. F. Çakır, M. Ürgen, D. H. Ross and D. R. Gabe, *Trans. Inst. Metal Finishing*, **76**, 5, 179 (1998)
32. F. Sertçelik, A. F. Çakır, M. Ürgen, D. Gabe and D. Ross, *Proc. Eurocorr'97*, **II**, p 297 (1997)
33. F. Sertçelik, A. F. Çakır, M. Ürgen, and D.R. Gabe, *Interfinish'2000*, (Submitted)
34. F. Sertçelik, *The Effect of Pretreatment and Thin Layer Sulfuric Acid AC Anodization of 6063 Aluminium Alloys on its Corrosion Resistance*, PhD Thesis, Technical University of Istanbul, Turkey, pp 126 (1998)
35. F. Mansfeld and M.W. Kendig, *Proceedings "Aluminium Surface Treatment"*, The Electrochemical Society Inc., p. 263, (1986)
36. J. Hitzig, K. Jüttner, W.J. Lorenz and W. Paattsh, *Corr. Sci.*, **24**, 11/12, 945 (1984)
37. B. Van Der Linden, H. Terryn, and J. Vereecken, *Journal of Appl. Electrochem.*, **20**, 79. (1990)
38. J. De Laet, J. Scheers, H. Terryn and J. Vereecken, *Electrochimica Acta*, **38**, 14, 2103 (1993)
39. C.M.A. Brett, *Corr. Sci.*, **33**, 12, 203 (1993)
40. C. Gudic J. Radosevic and M. Kliskic, *J. Appl. Electrochem.*, **26**, 1027 (1996)
41. C. A. Gervasi and J. R. Viche, *Electrochimica Acta*, **37**, 8, 1389 (1992)
42. W Paatsch, *Proceedings "Surface treatment of Aluminium"*, EAST-AIFM, p 87 (1991)
43. M. Ürgen, *Corros. Sci.*, **33**, 7, 1179 (1992)
44. B. Chatterjee and R. W. Thomas, *Trans. Inst. Metal Finishing*, **54**, 17 (1976)
45. A. J. Dowell, *Trans. Inst. Metal Finishing*, **65**, 147 (1987)
46. L. F. Mondolfo, *Aluminium Alloys: Structure And Properties*, Butterworths Press, London, 1976: p 67
47. O. Lunder and K. Nişancioğlu, *Corrosion Science*, **44**, 7, 414 (1987)
48. K. Nişancioğlu, *J. Electrochem. Soc.*, **137**, 1, 69. (1990)
49. H. H. Uhlig, *The Corrosion Handbook*, John Wiley and Sons, 1961: p 133
50. J. De Laet, J. Scheers, H. Terryn and J. Vereecken, *Proceedings Of EAST-AIFM Symposium on Surface Treatment Of Aluminium*, p 130 (1990)
51. G. R.T. Schueller, S.R. Taylor and E. E. Hajcsar, *J. Electrochem. Soc.*, **139**, 10, 2799 (1992)
52. J. Zahavi, H. Kerbel and O. Korotkina, *AES 71th Annual Conference*, (1984)